Quantifying the Sputtering Response of Graphitic Structures with Molecular Dynamics Simulations

IEPC-2022-592

Presented at the 37th International Electric Propulsion Conference
Massachusetts Institute of Technology, Cambridge, MA USA
June 19-23, 2022

Huy Tran[1] and Huck Beng Chew[2]
University of Illinois Urbana Champaign, Urbana, Il, 61801, USA

Carbon contamination of the electric propulsion (EP) facility through back sputtering is a well-known problem in EP testing, especially for high power EP devices. Specifically, sputtering of graphitic coatings on the testing chamber walls, followed by redeposition of these sputter contaminates on critical surfaces such as the chamber and thruster of EP engines can significantly influence ground-based EP thruster lifetime and performance predictions, since these carbon contaminates are not present in space environment. Here, we conduct large-scale, massively-parallel molecular dynamics (MD) simulations to quantify the sputtering rate of graphitic structures, while accounting for surface morphology effects, under Xe ion bombardment. We demonstrate that surface roughness significantly reduces the sputtering rate at ion incidence angles. By accounting for surface roughness effects, our MD predictions of the sputtering yield are in very good agreement with prior experiments.

I. Introduction

The need for an efficient, high-thrust space propulsion system to augment or replace traditional chemical propulsion systems is of great national importance, and is paramount to advancing space supremacy of the United States. One of the candidate propulsion system for NASA's Artemis program and human space flight missions on Mars is the Hall Thruster, which is a high power electric propulsion (EP) system. Even though EP has been an integral part of space exploration since the late 1990s, high power EP (>100 kW), such as Nuclear Electric Propulsion, remains largely an engineering concept due to insufficient correlation between ground-test results versus in-flight performance and wear. Because of the interaction between ground-based EP test facilities and thruster operations, the ground-based test measurements cannot adequately represent thruster operations under in-space environments, leading to significant uncertainties in performance and lifetime predictions. One major challenge is the presence of contaminants orignating from facility walls which interact with the thruster through back-sputtering, contaminant transport and redeposition [1]. To reduce these effects of facility back-sputtering, graphitic structures have traditionally been used to line the walls of the testing chamber. Nevertheless, at high ion energies (high eV), even pyrolytic graphite undergoes significant sputtering. The dispersion of these back-sputtered carbon species throughout the facility, and subsequent deposition on the carbon pole covers, center-mounted cathode, anode, and on boron nitride channels, leads to significant uncertainties in EP thrusters' lifetime and performance assessments.

Particle-In-Cell (PIC) models simulating the plasma environment can be used to elucidate the effects of carbon deposition on critical EP surfaces. These PIC models, however, require detailed information on the sputtering yield of a given graphitic structure as a function of the incident ion type (Xe, Ar, Kr), energy, and angle, as well as surface temperature and morphology [2,3]. The non-linear dependence of each of these parameters can be quite complex and contributes to a range of direct, binary, or collision cascade mechanisms that influence the sputtering rate. Semi-analytical theories have been proposed by Yamamura and others to estimate sputter yields for ion-elemental targets

[1] PhD Candidate, Aerospace Engineering, huydt2@illinois.edu
[2] Associate Professor, Aerospace Engineering, hbchew@illinois.edu.

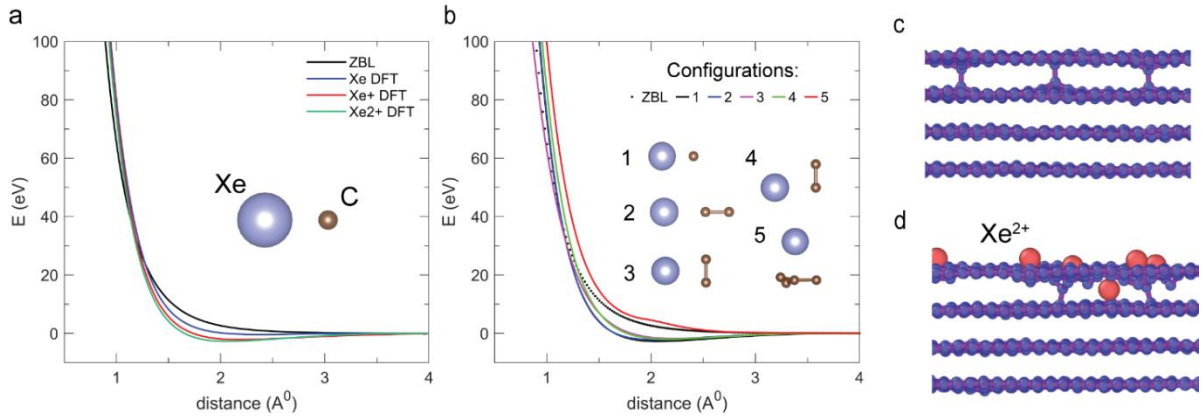

Fig. 1: Comparison between DFT (VASP) calculations and ZBL for potential vs atomic distance between: (a) Single Xenon and Carbon for various ionization of Xenon (b) Xe^{2+} with various configurations of carbon, inset: Schematics of carbon configurations (c) Xe deposition onto graphite surface at 70 eV (d) Xe^{2+} deposition onto graphite surface at 60 eV

(typically metallic alloys). However, these analytical formulations tend to underpredict experimental sputter yield [4–7], especially under the low ion energy values (100-1000 eV) expected in EP environments. In addition, these semi-empirical models cannot adequately capture the sputtering rates in covalently-bonded structures such as graphite, which undergo amorphization under ion bombardment. The reported sputtering rates for pyrolytic graphite are also found to be inconsistent among experimental studies in the literature, which have been alluded to the contributions of surface roughness effects at a higher length-scale [8,9].

In this work, we conduct large-scale, massively-parallel molecular dynamics (MD) simulations to predict the sputtering yield of graphitic structures under Xe ion bombardment. We quantify the sputtering mechanisms, type of sputterants, and the sputtering rate and energy, as a function of ion incidence angle. These MD results in turn are used to construct an analytical model to account for the added contributions of surface roughness at a higher scale. Our predictions are also compared against existing experiments in the literature.

II. Methodology

A. Atomistic simulations of pyrolytic graphite

MD simulations with well-calibrated interatomic potentials are well-suited to capture the detailed sputtering mechanisms, as well as to provide quantitative insights into the effects of incident angle and ion energy distributions on the sputtering rate. Our MD simulations will be performed using the classical MD simulator, LAMMPS. The interatomic interactions between Carbon and Carbon species will be governed by an Adaptive Intermolecular Reactive Empirical Bond Order (AIREBO) Potential, while the Ziegler-Biersack-Littmark (ZBL) potential governs the interaction between Xe inert gas ions as well as between Xe ions and carbon atoms [10,11]. This ZBL potential can only account for screened nuclear repulsion associated with high-energy collision between atoms and is deemed suitable when the nucleus interaction trumps over electron cloud interactions, which is expected at ion energies of 25 to 1000 eV [10]. Using Density Functional Theory (DFT) calculations with VASP, we have performed a series of validation studies demonstrating that this simple ZBL potential accurately captures the repulsive interaction and cut-off radius between Carbon and Xenon pair atom interactions (Fig. 1a and 1b) across various s, sp, and sp2 configurations of carbon (inset in Fig. 1b). We remark the presence of a small, additional attractive potential between carbon and positively-charged Xe ions (particularly Xe^{2+}). At

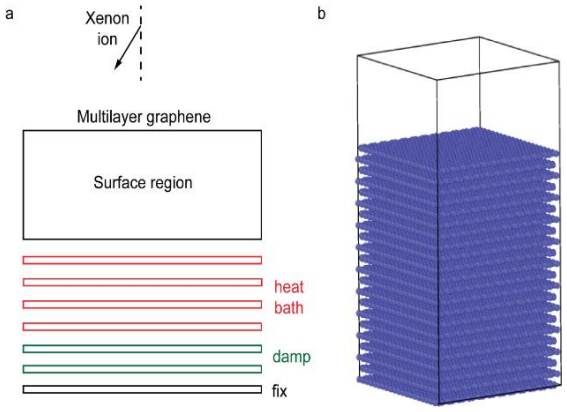

Fig. 2: (a) Schematic of the energetic bombardment of Xe ions on a multilayer graphene (b) Initial atomic configuration of 22 graphene layers for Xe bombardment at 700 eV.

low ion energies of 20 – 70 eV, this additional attractive interaction when incorporated in our MD simulations contributes to increased sticking of Xe ions on graphitic surfaces, as shown in Fig. 1d. In the absence of this attractive component, the Xe atoms instead bounces off the graphitic surface (Fig. 1c).

In our MD simulations, we conduct Xe ion bombardment of multilayer graphene with ABA stacking oriented normal to the vertical (z) axis (Fig. 2a). The simulation box is periodic in the in-plane (x-y) directions with the dimensions of 51.12 x 49.19 nm^2. In our simulation box (Fig. 2a), we fix the bottom graphene layer throughout our simulations and designate the next two layers above as the damping layer, followed by four heat bath layers. Depending on the Xe ion incidence energy and angle, we include multiple graphene layers (22 in the case of Xe ion energy of 700 eV in Fig. 2b) above to ensure that the incident Xe ion remains trapped within the active graphene layers above this heat bath region.

Prior to initiating the bombardment sequence, we subject the multilayer graphene system to an NVT ensemble maintained at a temperature of 400 K by a Berendsen thermostat for 30 ps, which is a typical surface temperature from a beam dump experiment [12,13]. For each simulation step, we deposit one Xe ion randomly above the graphitic surface with a time step of 0.1 fs; each Xe ion has initial velocity in the -z, +x, +y direction corresponding to the kinetic energy of 25 – 1000 eV and an incidence angle of between 0° and 75°. After initiating this deposition process, we equilibrate the entire system without a thermostat for the first 1 ps to resolve the initial impact dynamics. Thereafter, we switch on the thermostat in the heat-bath region and set it to the target temperature of 400 K for the next 20 ps, before quenching the surface layer to 400 K for a further 20 ps. The equilibration and the quenching process have time step of 1 fs. After each bombardment cycle, we capture the species (either Xe or C) that escape the simulation box, noting the species type, energy, and trajectory. The entire bombardment sequence is then repeated until the sputtering yield, as defined by the ratio of sputtered C atoms versus incoming Xe ions, has attained a steady-state.

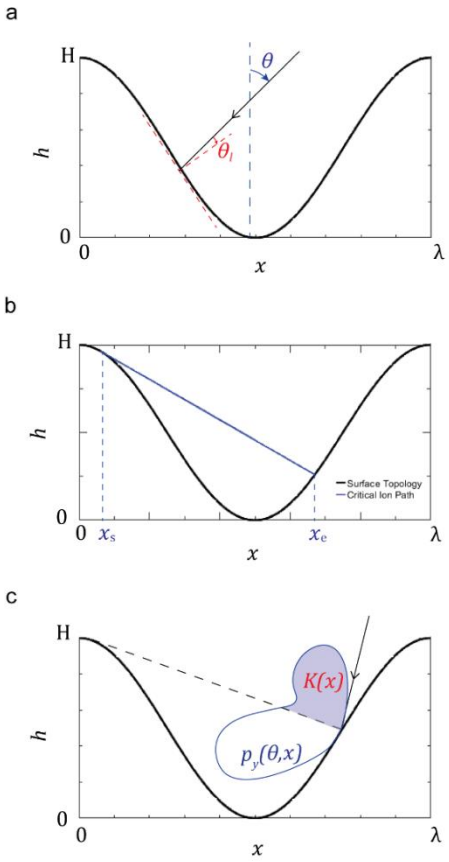

Fig. 3: Surface morphology defined by $h(x) = \frac{H}{2}\cos\left(2\pi\frac{x}{\lambda}\right) + \frac{H}{2}$ (a) the parameters definition (b) non-expose surface to the incoming ion, indicates in the region where $x_s < x < x_e$ (c) geometric factor accounts for sputtering atom direction

B. Analytical Model

The time-accelerated MD simulations are computationally expensive and require high performance computing (HPC) facilities. Therefore, only a finite number of atoms can realistically be modeled, restricting our simulation box dimensions to several tens of nanometers. Comparatively, the surface roughness have length-scales on the order of microns. To bridge these length-scales, we represent the surface morphology by a cosine function of amplitude $H/2$ and wavelength λ

$$h(x) = \frac{H}{2}\cos\left(2\pi\frac{x}{\lambda}\right) + \frac{H}{2} \qquad (1)$$

For simplicity, we assume that both H and λ remain constant during the bombardment process. Because of shadowing effect, a region ($x_s < x < x_e$ in Fig. 3b) of the surface will not be exposed to the incoming ion. In the exposed region, the emission of sputterants follows a probability density function (pdf), $p_y(\theta, x)$ computed from MD simulations. Depending on the morphology, only a proportion of the sputterants (shaded region in Fig. 3c) can escape the calculation domain, as characterized by a multiplier $K(x)$ with $0 \le K(x) \le 1$ obtained from MD simulations; the limits $K(x) = 0$ and 1 denotes the full redeposition and emission of all sputtered atoms.

The effective yield, Y_{eff}, can be expressed as:

$$Y_{eff}\left(\frac{H}{\lambda}, \theta\right) = \frac{1}{\lambda}\int_0^{\lambda} K(x) Y_c\big(\theta_l(x)\big) U(x) dx \qquad (2)$$

$$U(x) = \text{stp}(-x - x_s) + \text{stp}(x - x_e) \qquad (3)$$

where $\text{stp}(x)$ is a unit step function, θ is the ion incident angle measuring from the normal vector at $x = \lambda/2$, $\theta_l(x)$ is the local ion incident angle with respect to the normal vector of an infinitesimal surface locates at x (Fig. 1a), and $Y_c\big(\theta_l(x)\big)$ is the principle yield. For a perfectly smooth

surface, i.e. $\frac{H}{\lambda} = 0$, we obtain $Y_{eff} = Y_c$. For . $\frac{H}{\lambda} > 0$, we solve (2) numerically by discretizing the domain $0 \leq x \leq \lambda$ into elements, i, each of size, Δx^i, with a constant incoming ion flux within each Δx^i.

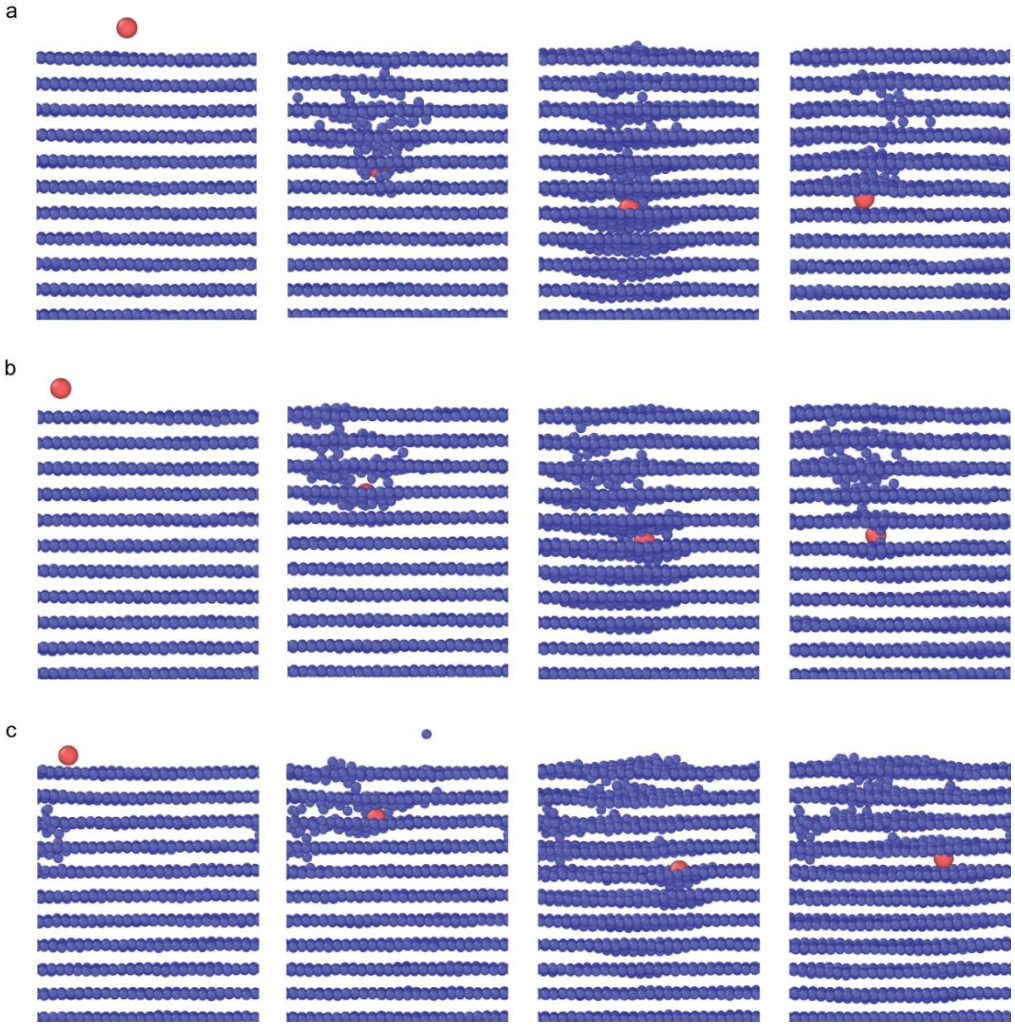

Fig. 4: MD Simulation snapshot of the first initial Xenon bombardment process with incidence energy of 700 eV as Xenon moving into the multilayered graphene (from left to right) at (a) $\theta = 0^0$ (b) $\theta = 30^0$ (c) $\theta = 45^0$

III. Case study: Xenon bombardment at 700 eV incidence energy

A. MD simulations result

Figure 4 shows snapshots of the initial penetration sequence of a Xe ion into multi-layer graphene with an incidence energy of 700 eV and at three incidence angles: 0°, 30°, 45°. In all three cases, the penetration of Xe ions causes some disruption to the atomic arrangement of C atoms in its path, and the Xe ion eventually remains trapped within the C layers, albeit at different penetration depths depending on the ion incidence angles. The process results in the

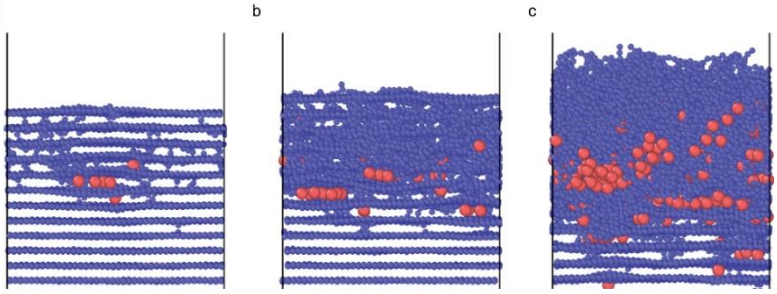

Fig. 5: Carbon structure transformation under Xenon bombardment at 700eV and $\theta = 30^0$.

emission of a sputtered C atom in the case of Fig. 4c. With increasing fluence, graphitic structure becomes more amorphous and porous (Fig. 5). Due to the high percentage of weaker sp rather than stronger sp2 type bonding, the sputtering yield inceases (Fig. 6), until the structure is completely amorphized allowing the sputtering yield to reach its steady-state.

B. Effect of surface morphology on sputtering yield

Our MD simulations above are used to quantify the steady-state sputtering yield of amorphous graphite under Xe ion bombardment at 700 eV across four different incident angles $0°, 30°, 45°, 60°$ to compute $Y_c(\theta)$ and $K(x)$ in (2). We consistently observe steady state sputtering at fluence of 10^{15} ion/cm^2 across these four ion incidence angles. Figure 7a shows the sputtering count evolution as a function of Xe flux, and we summarize the steady-state sputtering yield from our simulations in Table 1. Our simulations show good agreement with predictions from TRIM models across all four ion incidence angles. Interestingly, our MD predictions are also in good agreement with experimental results at low incidence angles $(0°, 30°)$ but tend to overestimate the sputtering yield at high incidence angles $(45°, 60°)$. These discrepancies can be attributed to surface roughness effects. Figure 7b shows the evolution of the steady state sputtering rate as a function of the roughness amplitude $\frac{H}{\lambda}$ based on (2). Observe that for $\frac{H}{\lambda} \leq 0.1$, the sputtering yield decreases by nearly two-fold at an ion incidence angle of 60°, but slightly increases at lower incidence angles of $0°, 30°, 45°$. For $0.1 \leq \frac{H}{\lambda} \leq 0.5$, the sputtering yield increases slightly at incidence ion angle of 0° but decreases for other angles. Our sputtering yield predictions are in very good agreement with prior experiments (see Table 1), at $\frac{H}{\lambda} = 0.2$ to 0.25, which is representative of the morphology of graphitic surfaces as quantified by atomic force microscopy experiments .

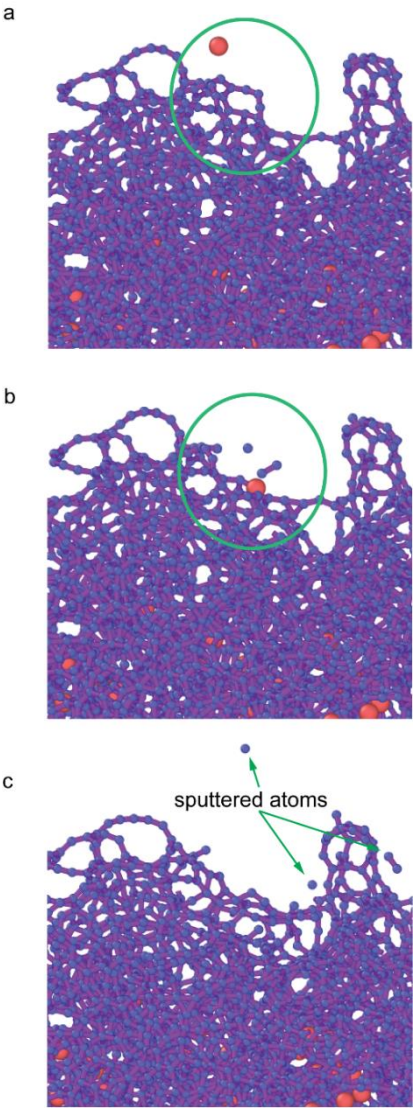

Fig. 6: Representative sputtering mechanism once the graphitic structure has fully transformed into amorphous carbon

IV. Conclusion and Future Works

In conclusion, we have obtained a first-order estimate of the sputtering yield of carbon from a graphitic surface subjected to Xe ion bombardment, where we account for surface roughness effects. We demonstrate that the presence of surface roughness significantly reduces the sputtering rate at high ion incidence angles. By accounting for surface roughness effects, our predictions of the sputtering yield are in almost perfect agreement with prior experiments. Future extensions of this model can include the effects of surface evolution resulting from the sputtering and re-deposition of carbon species.

Table 1: Sputtering yield comparing the experiments with four different H/λ

Angle (^{0})	**William** [14]	**Tartz** [9]	$\frac{H}{\lambda} = 0$ (MD)	$\frac{H}{\lambda} = 0.1$	$\frac{H}{\lambda} = 0.2$	$\frac{H}{\lambda} = 0.25$
0	0.196	0.25	0.118	0.190	0.226	0.235
30	0.366	0.39	0.358	0.391	0.382	0.343
45	0.394	0.52	0.674	0.748	0.505	0.387
60	0.421	0.68	1.630	1.094	0.642	0.496

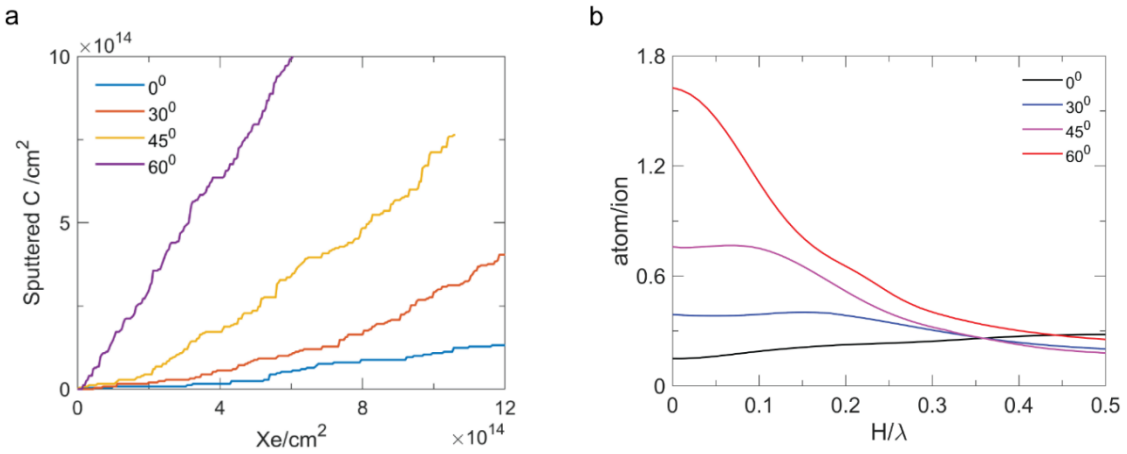

Fig. 7: (a) Carbon sputtered evolution with incoming Xenon flux (b) Sputtered yield changes as a function of H/λ across four different angles

Acknowledgments

This work is supported by NASA through the Joint Advanced Propulsion Institute, a NASA Space Technology Research Institute, grant number 80NSSC21K1118. The use of the Extreme Science and Engineering Discovery Environment (XSEDE) through allocations TG-PHY220010, TG-MAT210010, and TG-MAT210031 are gratefully acknowledged.

References

[1] Polk, J., Duchemin, O., Ho, C., and Koel, B. "The Effect of Carbon Deposition on Accelerator Grid Wear Rates in Ion Engine Ground Testing." *undefined*, 2000.

[2] Kim, S.-P., and Lee, K.-R. "Molecular Dynamics Study of Ballistic Rearrangement of Surface Atoms during High Energy Ion Bombardment on Pd (001) Surface." Vol. 1, 2008, p. 5.

[3] Kim, S.-P., Chew, H. B., Chason, E., Shenoy, V. B., and Kim, K.-S. "Nanoscale Mechanisms of Surface Stress and Morphology Evolution in FCC Metals under Noble-Gas Ion Bombardments." *Proceedings of the Royal Society A: Mathematical, Physical and Engineering Sciences*, Vol. 468, No. 2145, 2012, pp. 2550–2573. https://doi.org/10.1098/rspa.2012.0042.

[4] Yamamura, Y., and Shindo, S. "An Empirical Formula for Angular Dependence of Sputtering Yields." *Radiation Effects*, Vol. 80, Nos. 1–2, 1984, pp. 57–72. https://doi.org/10.1080/00337578408222489.

[5] Yamamura, Y., and Tawara, H. "Energy Dependence of Ion-Induced Sputtering Yields From Monatomic Solids at Normal Incidence." *Atomic Data and Nuclear Data Tables*, Vol. 62, No. 2, 1996, pp. 149–253. https://doi.org/10.1006/adnd.1996.0005.

[6] Eckstein, W., and Preuss, R. "New Fit Formulae for the Sputtering Yield." *Journal of Nuclear Materials*, Vol. 320, No. 3, 2003, pp. 209–213. https://doi.org/10.1016/S0022-3115(03)00192-2.

[7] Sigmund, P. Sputtering by Ion Bombardment Theoretical Concepts. In *Sputtering by Particle Bombardment I* (R. Behrisch, ed.), Springer Berlin Heidelberg, Berlin, Heidelberg, 1981, pp. 9–71.

[8] Oyarzabal, E., Doerner, R. P., Shimada, M., and Tynan, G. R. "Carbon Atom and Cluster Sputtering under Low-Energy Noble Gas Plasma Bombardment." *Journal of Applied Physics*, Vol. 104, No. 4, 2008, p. 043305. https://doi.org/10.1063/1.2968549.

[9] Tartz, M. "Pyrolytic Graphite and Carbon-Carbon Sputter Behaviour under Xenon Ion Incidence." *the International Electric Propulsion Conference*, 2005, p. 10.

[10] Ziegler, J. F., and Biersack, J. P. The Stopping and Range of Ions in Matter. In *Treatise on Heavy-Ion Science: Volume 6: Astrophysics, Chemistry, and Condensed Matter* (D. A. Bromley, ed.), Springer US, Boston, MA, 1985, pp. 93–129.

[11] Stuart, S. J., Tutein, A. B., and Harrison, J. A. "A Reactive Potential for Hydrocarbons with Intermolecular Interactions." *The Journal of Chemical Physics*, Vol. 112, No. 14, 2000, pp. 6472–6486. https://doi.org/10.1063/1.481208.

[12] Ermilov, A. N., Eroshenkov, V. F., Novichkov, D. N., Kovalenko, Yu. A., Sapronova, T. M., Chernyshev, T. V., and Shumilin, A. P. "Oscillations of the Hall Current in a Hall Thruster with an Anode Layer." *High Temperature*, Vol. 52, No. 3, 2014, pp. 360–365. https://doi.org/10.1134/S0018151X14030109.

[13] Rosenberg, D., and Wehner, G. K. "Sputtering Yields for Low Energy He^+-, Kr^+-, and Xe^+-Ion Bombardment." *Journal of Applied Physics*, Vol. 33, No. 5, 1962, pp. 1842–1845. https://doi.org/10.1063/1.1728843.

[14] Williams, J., Johnson, M., and Williams, D. Differential Sputtering Behavior of Pyrolytic Graphite and Carbon-Carbon Composite Under Xenon Bombardment. Presented at the 40th AIAA/ASME/SAE/ASEE Joint Propulsion Conference and Exhibit, Fort Lauderdale, Florida, 2004.